

Computer Aided Diagnosis of Thyroid Cancer Using Image Processing Techniques

Massoud Sokouti¹, Mohsen Sokouti^{2*}, and Babak Sokouti^{3*}

¹Nuclear Medicine Research Center, Mashhad University of Medical Sciences, Mashhad, Iran.

^{2*}Department of Cardiothoracic Surgery, Tabriz University of Medical Sciences, Tabriz, Iran.

^{3*}Biotechnology Research Center, Tabriz University of Medical Sciences, Tabriz, Iran.

Summary

One of the mathematical based techniques used for processing the medical images in order to identify the irregularity properties of these images is employing different types of Image processing algorithms. Detecting these abnormalities in terms of their risk of malignancy such as tumors in thyroid gland is of a major importance in nuclear medicine which is known as cold nodules. In this study, the radioisotope image of thyroid gland is used for extracting the cold nodules based on hot nodule extraction. For this purpose, two routes are employed which will be unified later for nodule extraction through a simple intelligent system. At First, the gray level of blue channel of the target image is mapped from range of [0,1] to [1,0] that a portion of the resulted image will be selected according to a predefined threshold. Second, the color image will be transformed into gray scale which will be then enhanced by circular average filtering and highlighting the intensity methods. Moreover, thresholding stage will also be applied to the obtained image in the second approach. After all both resulted images will be added and mapped will be then from range of [0,1] to [1,0] which will be ready for feature extraction using the simple hill climbing methodology. The results showed that after executing the process for hundred times the best area for cold nodule will be identified with high accuracy. In conclusion, it has been shown that by using image processing technique along with a simple intelligent system such as hill climbing algorithm, one can achieve the highest performance (i.e., accuracy of 0.9896) in detecting the malignancy in several medical related images.

Key words:

Image processing; Thyroid Cancer; Cold Thyroid Nodules; Hill climbing; Feature Extraction.

1. Introduction

The thyroid gland is located in front of larynx, under Adam's apple in the neck. This gland has two lobes with a butterfly shape. Thyroid gland is one of the endocrine glands with the ability of producing thyroid hormones. The thyroid gland with the help of thyroid hormones controls heart rate regulation, weight, body temperature, and blood pressure. Also, It can influence the childhood intelligence and growth, as well as the adults metabolism and secreting vital hormones such as levothyroxine and triiodothyronine [1-5]. Based on the literature reports, the

incidence rate of affected patients with malignant thyroid nodules and hence the thyroid cancer in children is more than adults however, the recurrence rate is close to 40 percent[6, 7]. This is mostly due to the geographical, regional and nutritional issues which results in varying thyroid disorders[8]. Therefore, determining malignancy or any types of abnormalities in the thyroid nodules from radioisotope images of thyroid gland is of much interest, however, several image processing and intelligent techniques on types of images including ultra-sonography (USG), single photon emission computed tomography (SPECT) and planar scintigraphy using neural networks fuzzy and genetic algorithm based approaches with varying performances[3].

The most well-known application of image processing technique in medical sciences is to reveal the specific patterns of images for determination or more investigation where detection of objects is of interest is of high priority. This technique has been widely used for diagnosing diseases such as cervical, lung, thyroid, and breast cancers to mention a few[9-15]. And hence, these can be implemented via various algorithms for the sake of processing the medical images [16, 17]. For diagnosing thyroid nodules, there are some imaging technologies to be considered which may include the magnetic resonance imaging (MRI), radiology, radioactive iodine scan, computed tomography and ultra sonography (USG)[17], and ultrasound [18]. Among them, we studied radioactive iodine scan of thyroid due to the high accuracy and resolution of the images which are the initial requirements for any image processing methodologies.

Considering the advanced development in molecular imaging technologies, diagnosis and treatment of thyroid nodules can be dramatically improved. Moreover, molecular imaging technology carried out by the radioactive iodine uptake can be used widely for thyroid nodules treatment [19]. Thyroid uptakes radioactive iodine can be appeared in three forms including hot, warm, and cold nodules. Due to the higher risks of malignancy, diagnosis of cold nodules is very important [20]. However, in the case of hot nodules the physicians are recommended to perform additional tests as these nodules are mostly considered as benign.[21]. Although, one of the recent studies orally presented in an Iranian national conference

*Corresponding Authors: sokouti.mohsen@yahoo.com; b.sokouti@gmail.com; sokoutib@tbzmed.ac.ir

Manuscript received April 5, 2018

Manuscript revised April 20, 2018

(i.e., 8th Iranian conference on electrical and electronic engineering) had conducted a pilot study on these types of images in 2016 [22], however, in the current study, a rigorous and efficient approach for image pre-processing has been developed. The aim of this study is to take the advantage of image processing techniques which is followed by an algorithmic flowchart to detect qualitatively the thyroid cold nodules in radioactive images. To the best of authors' knowledge, this study is the first to study the thyroid cold nodules carried out based on novel approaches using thyroid radioactive images as well as other newly used image processing algorithms. Additionally, we believe that the appropriate selection of preprocessing techniques can be effective in increasing the performance of diagnosis intelligent system and the same can be true for properties of a good classifier as confirmed in the ultrasound research [18].

2. Materials and Methods

For constructing the image dataset for input of the implemented image processing procedure, 200 RGB thyroid radioactive images were used. The first step of the current image processing approach for detecting cold nodules in thyroid radioactive images is to perform pre-processing to enhance the input images for further analyses. The image pre-processing or image enhancement step was done to eliminate any types of existing noises, corruption or interference or in other words enhancing and making the images for better processing outcomes. In this step, combination of several algorithms was applied. First of all, a two way procedure according to Fig 1 originating from the original image was designed where both grey scale as well as grey level of blue channel of the images play important roles to carry on the next steps due to the characters of the target images environment. The reason behind taking the advantage of grayscale of the images was simply that the color images were more complex models while compared to grayscale ones for decreasing the dimensional features and computational costs. The route that was started by the extracted grey level of blue channel image was continued by logical negation (to enhance the contrast) and thresholding (segmentation) approaches. Whereas the routed started by the converted image in to grey scale mode, went on by performing the circular average 2D filter which smoothens along diagonals rather than rows and columns to enhance the image, highlighting the region, and thresholding the images. These two routes would be merged by a logical summation and then, the logical negation would be applied to the resulted summed image. The second step that was done above is the image segmentation which means to divide and segment the enhanced image by thresholding

algorithms with the same thresholding algorithms and settings.

The last step in this procedure was feature extraction where finding the region of interest (ROI)(i.e., cold nodules) was carried out using hill climbing algorithm which had low computational costs while compared to the genetic algorithms (GAs). For achieving the best results, this algorithm would be run hundred times on the final image to find the ROI with the highest number of white pixels.

The schematic procedure shown in Fig 1 was implemented and programmed in MatlabR2013a. The computer system used for nodule identification had the hardware specifications with CPU Core i5, 6GB RAM, and 1TB hard disk.

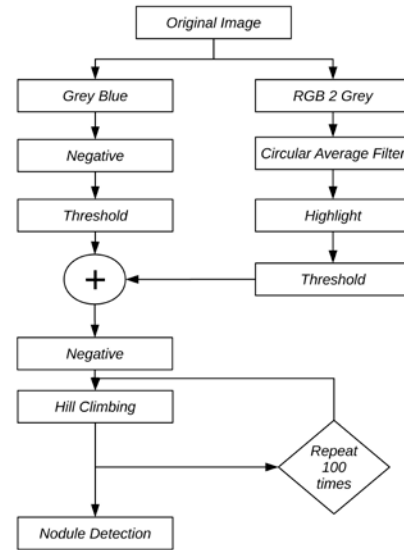


Fig1. Flowchart of the nodule extraction method consisting of pre-processing (image enhancement), segmentation, feature extraction and nodule detection.

For assessing the performance of the proposed procedure, Matthew's correlation coefficient, accuracy, sensitivity, specificity, and F Score measurement criteria [23] were used using the extracted region of interest and the manual section of the region (known as gold standard).

$$MCC = \frac{TP \times TN - FP \times FN}{\sqrt{(TP+FP)(TP+FN)(TN+FP)(TN+FN)}} \quad (1)$$

$$Accuracy = \frac{TP+TN}{TP+TN+FP+FN} \quad (2)$$

$$Sensitivity = \frac{TP}{TP+FN} \quad (3)$$

$$Specificity = \frac{TN}{TN+FP} \quad (4)$$

$$F\ Score = \frac{2TP}{2TP+FP+FN} \quad (5)$$

3. Results and discussion

3.1. Image Enhancement

At the first step, the image enhancement generally known as image pre-processing is applied on the images to improve the perception of images data set for automatic pattern detection via image processing techniques. In a two route procedure for taking advantage of both grey distribution of blue channel (dark) and grey scale of the images, the output of each step is illustrated in Fig 2. The original input image is shown in Fig 2a, whereas figures 2b and 2c show the converted form of the sample image in terms of extracted grey distribution of blue channel and the converted grey scale. Spatial and frequency domain methods are the known image enhancement techniques [16, 24]. Considering the left route (i.e., extracted grey distribution of blue channel), only logical negation is performed (Fig 2d) and the other route for performing the image enhancement, a 2D filter (circular averaging filter) is applied followed by highlighting the intensity. The results of these two steps are shown in figures 2e and 2g, respectively.

3.2. Image Segmentation

Image segmentation is an inseparable part of any image description and recognition technique which can divide image into black and white regions by using pre-defined threshold values[25]. Detection of abnormalities like tumors and tissues classification can be carried out by image segmentation techniques. It labels every pixel of image so the pixels with the same label similar characteristics. This is commonly done for making the medical images easy to analyze and interpret [26]. Discontinuity and similarity are properties of image segmentation which are based on edge and histogram thresholding, respectively [24]. Thresholding is one of the most important methodologies in image segmentation during the past twenty years. After applying the thresholding on the resulted images, the pixels will change into logical (1 or 0). Thresholding can increase the speed of processing and reduce the space that is needed to store the image [27]. Figures 2f and 2h are the results of the previous stages of image enhancement (figures 2d and 2g) after thresholding procedure.

3.2. Feature Extraction for Nodule Detection

After applying image enhancement and image segmentation, two other techniques namely logical summation and negation are applied where their output are shown in figures 2i and 2j. In this step, one may only make the image more clear however, it's not

enough since the ROI has not been found automatically. Therefore, it is essential to implement an algorithm to determine the cold nodules (the biggest white regions) which are the regions of interest (ROIs). For this purpose, a simple hill climbing algorithm followed by hundred times of consecutive runs will be performed in order to be sure that the heuristic methodology will finally find the ROI with largest area in terms of number of pixels.

Other literature articles have used several intelligent systems methodologies such as artificial neural networks (ANNs), genetic algorithm (GA), Fuzzy Support Vector Machines (F-SVM) and Support Vector Machines (SVM) to mention a few [17, 28, 29]. A recent study employed extreme learning machine (ELM) approach for diagnosing benign and malignant thyroid tumors based on the features of ultrasound images (i.e., echogenicity, calcification, margin, composition, and shape via ReliefF method [30]) which achieved 87.7% accuracy, 78.9% sensitivity, and 94.6% specificity [18], and hence they are not comparable with the current approach which is different in terms of target images, image processing techniques and automated intelligent system. The hill climbing algorithm is an optimization technique, similar to genetic algorithm with less computational costs and complexity in comparison to seeded region growing [31] (used mostly for multiple region extraction), which also works with random numbers and finds local optimums [32]. By applying the hill climbing algorithm on Fig 2j which had shown good results in other studies as well [33], a random point will be chosen from white regions of the image. And, the developed algorithm starts to count the white pixels from that point to North, North West, North East, South, South West, South East of the image until it faces the black regions. The approach is repeated this procedure one hundred times and finds the ROI with the highest count numbers as the cold nodule place. The best result is illustrated in Fig 2k. In this study, the extracted region will be the only qualitative feature for diagnosing the cold nodules. However, the structures of cold and hot nodules are different and can be easily discriminated using the proposed algorithm.

By applying the developed procedure including the image processing techniques and intelligent system, on the target images, the results showed that a high performance has been achieved that is summarized in Table 1. The average of the overall performance for Mathew's correlation coefficient (MCC), Accuracy, Sensitivity, Specificity, and F score are 0.83092, 0.9896, 0.8, 0.997, and 0.83405, respectively which is an indication for the high performance of the proposed methodology. The

obtained results for the new proposed method are indicative of the fact that even if the same region growing hill climbing method is employed for the final step as in our previous study [22], however, due to the different initial pre-processing algorithms, better results have been achieved in the current study.

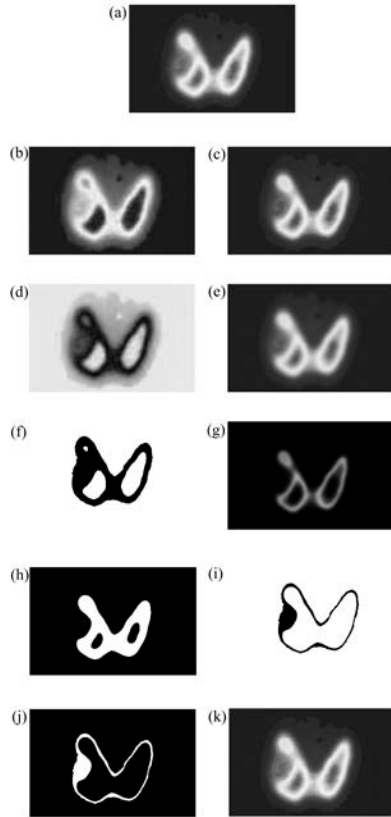


Fig 2.The results of each step in the Fig 1 flowchart. (a) Original RGB thyroid radioactive image illustrated in grey scale mode (b) Extracted grey distribution of blue channel of the original RGB image (c) Converted RGB image into grey scale (d) Logical negation of grey distribution of blue channel (transformed negative form) (e) Circular averaging 2D-filter of grey scale image (f) Thresholding of the negation form (g) Highlighting the region (h) Thresholding of highlighted region (i) Logical summation of (g) and (h) (j) Logical negation of the resulted image (k) Revealed thyroid cold region by hundred times of hill climbing.

Table 1- List of performance results on cold nodule detection in terms of Matthew's correlation coefficient (MCC), Accuracy, Sensitivity, Specificity, and F score.

IMG	MCC	Accuracy	Sensitivity	Specificity	F-Score	IMG	MCC	Accuracy	Sensitivity	Specificity	F-Score
1	0.8152	0.9838	0.7322	0.9969	0.8175	101	0.809	0.9923	0.825	0.9958	0.8126
2	0.8565	0.9873	0.77	0.9986	0.8571	102	0.818	0.993	0.8052	0.9968	0.8216
3	0.8975	0.9907	0.8494	0.9981	0.9006	103	0.861	0.9946	0.8408	0.9978	0.863
4	0.8283	0.9849	0.745	0.9974	0.8302	104	0.804	0.9919	0.8387	0.9951	0.8074
5	0.8772	0.989	0.8034	0.9987	0.8787	105	0.806	0.9921	0.8375	0.9952	0.8095
6	0.9054	0.9914	0.8546	0.9985	0.908	106	0.804	0.9922	0.8121	0.9959	0.8081
7	0.8661	0.9879	0.8245	0.9964	0.8709	107	0.811	0.9926	0.8038	0.9965	0.8147
8	0.8477	0.9865	0.7372	0.9996	0.8447	108	0.796	0.9918	0.8193	0.9953	0.8002
9	0.888	0.9899	0.8387	0.9977	0.8913	109	0.86	0.9947	0.8149	0.9984	0.8613
10	0.8498	0.9867	0.7581	0.9986	0.8498	110	0.805	0.9924	0.7981	0.9964	0.8083
11	0.8617	0.9876	0.8028	0.9972	0.8653	111	0.786	0.9917	0.7721	0.9962	0.7895
12	0.8992	0.9909	0.8406	0.9987	0.9014	112	0.78	0.9914	0.7739	0.9959	0.7838
13	0.8358	0.9854	0.772	0.9965	0.8399	113	0.797	0.992	0.7999	0.996	0.8015
14	0.8485	0.9864	0.8002	0.9961	0.8536	114	0.813	0.9927	0.8061	0.9965	0.8167
15	0.7815	0.9811	0.6855	0.9965	0.7826	115	0.787	0.9917	0.7819	0.996	0.7909
16	0.8555	0.9871	0.784	0.9977	0.858	116	0.825	0.9933	0.8002	0.9973	0.8282
17	0.8792	0.9891	0.8173	0.9981	0.8818	117	0.782	0.9915	0.7805	0.9958	0.7867
18	0.8343	0.985	0.7981	0.9948	0.8408	118	0.872	0.9951	0.8393	0.9983	0.8733
19	0.8553	0.987	0.807	0.9964	0.8601	119	0.796	0.9918	0.8161	0.9954	0.8001
20	0.8596	0.9875	0.7861	0.998	0.8617	120	0.814	0.9926	0.8236	0.9961	0.8181
21	0.8847	0.9896	0.8351	0.9976	0.8882	121	0.795	0.9917	0.8128	0.9954	0.7988
22	0.8843	0.9896	0.8192	0.9985	0.8865	122	0.821	0.9928	0.8405	0.9959	0.8241
23	0.776	0.9807	0.6677	0.9971	0.7748	123	0.821	0.9928	0.8405	0.9959	0.8241
24	0.8438	0.9862	0.7518	0.9984	0.844	124	0.783	0.9915	0.7828	0.9958	0.7877
25	0.8943	0.9904	0.8563	0.9974	0.8982	125	0.838	0.9937	0.8287	0.9971	0.8413
26	0.8975	0.9907	0.8494	0.9981	0.9006	126	0.809	0.9923	0.825	0.9958	0.8126
27	0.8151	0.9839	0.6882	0.9994	0.8093	127	0.827	0.9932	0.8266	0.9966	0.8303
28	0.868	0.9882	0.7941	0.9983	0.8698	128	0.814	0.9926	0.8236	0.9961	0.8181
29	0.8975	0.9907	0.8494	0.9981	0.9006	129	0.814	0.9926	0.8236	0.9961	0.8181
30	0.8866	0.9896	0.8595	0.9964	0.8914	130	0.84	0.9939	0.8166	0.9975	0.8429
31	0.8927	0.9903	0.8326	0.9985	0.895	131	0.795	0.9917	0.8128	0.9954	0.7988
32	0.8335	0.9854	0.7308	0.9987	0.8322	132	0.78	0.9914	0.7739	0.9959	0.7838
33	0.8688	0.9882	0.8055	0.9978	0.8717	133	0.792	0.9916	0.8157	0.9952	0.7961
34	0.8981	0.9908	0.8309	0.9991	0.8995	134	0.783	0.9915	0.7828	0.9958	0.7877
35	0.8679	0.9882	0.8036	0.9978	0.8707	135	0.806	0.9922	0.8263	0.9956	0.8099
36	0.7924	0.9819	0.7123	0.9959	0.7958	136	0.837	0.9937	0.826	0.9971	0.8403
37	0.8141	0.9837	0.7224	0.9974	0.8151	137	0.806	0.9922	0.8263	0.9956	0.8099
38	0.8647	0.9879	0.7846	0.9986	0.8658	138	0.804	0.9919	0.8387	0.9951	0.8074
39	0.8791	0.9891	0.8217	0.9978	0.8821	139	0.83	0.9932	0.8453	0.9962	0.8329
40	0.8568	0.9872	0.7853	0.9978	0.8593	140	0.8	0.992	0.8117	0.9957	0.8036
41	0.813	0.9836	0.7224	0.9973	0.8142	141	0.837	0.9937	0.8171	0.9973	0.8396
42	0.756	0.979	0.6668	0.9953	0.7589	142	0.824	0.993	0.8263	0.9965	0.8272
43	0.8847	0.9896	0.8351	0.9976	0.8882	143	0.852	0.9943	0.8268	0.9978	0.8542
44	0.8274	0.9845	0.7838	0.9949	0.8336	144	0.806	0.9921	0.8375	0.9952	0.8095
45	0.8163	0.9838	0.7479	0.9961	0.8205	145	0.804	0.9919	0.8387	0.9951	0.8074
46	0.8841	0.9895	0.8361	0.9975	0.8877	146	0.795	0.9918	0.813	0.9954	0.7993
47	0.8619	0.9876	0.7974	0.9976	0.8649	147	0.821	0.9928	0.8405	0.9959	0.8241
48	0.8982	0.9908	0.8468	0.9983	0.901	148	0.816	0.9927	0.8217	0.9962	0.8192
49	0.8049	0.9831	0.6861	0.9986	0.801	149	0.791	0.9918	0.7837	0.9961	0.7946
50	0.9054	0.9914	0.8546	0.9985	0.908	150	0.846	0.9941	0.8201	0.9977	0.8489
51	0.8302	0.9848	0.7815	0.9954	0.836	151	0.809	0.9923	0.825	0.9958	0.8126
52	0.877	0.989	0.7939	0.9992	0.8773	152	0.793	0.992	0.7792	0.9964	0.7973
53	0.8167	0.9837	0.7532	0.9958	0.8214	153	0.796	0.9918	0.8161	0.9954	0.8001
54	0.85	0.9867	0.7651	0.9983	0.851	154	0.789	0.9917	0.7891	0.9959	0.7932
55	0.8857	0.9897	0.8234	0.9984	0.8881	155	0.788	0.9917	0.788	0.9959	0.7924
56	0.885	0.9896	0.83	0.998	0.8881	156	0.834	0.9937	0.7983	0.9977	0.8363
57	0.8372	0.9855	0.7715	0.9967	0.8409	157	0.83	0.9932	0.8453	0.9962	0.8329
58	0.9054	0.9914	0.8546	0.9985	0.908	158	0.826	0.993	0.8399	0.9962	0.8292

59	0.8344	0.9852	0.7744	0.9963	0.8389	159	0.811	0.9926	0.8038	0.9965	0.8147
60	0.8716	0.9885	0.8117	0.9977	0.8747	160	0.782	0.9915	0.7805	0.9958	0.7867
61	0.8428	0.986	0.778	0.9969	0.8465	161	0.815	0.9927	0.8165	0.9963	0.8183
62	0.8218	0.9842	0.7569	0.9961	0.8262	162	0.788	0.9917	0.7822	0.996	0.7917
63	0.8866	0.9896	0.8595	0.9964	0.8914	163	0.804	0.9919	0.8387	0.9951	0.8074
64	0.8793	0.9891	0.8148	0.9983	0.8817	164	0.818	0.993	0.8052	0.9968	0.8216
65	0.7815	0.9811	0.6855	0.9965	0.7826	165	0.852	0.9943	0.8268	0.9978	0.8542
66	0.8645	0.9877	0.8218	0.9964	0.8693	166	0.818	0.9928	0.8262	0.9962	0.8217
67	0.8765	0.9889	0.8144	0.998	0.8792	167	0.822	0.993	0.8215	0.9966	0.826
68	0.8072	0.983	0.7417	0.9956	0.8121	168	0.78	0.9914	0.7739	0.9959	0.7838
69	0.8645	0.9877	0.8218	0.9964	0.8693	169	0.789	0.9917	0.789	0.9959	0.7936
70	0.8045	0.9827	0.7417	0.9953	0.8097	170	0.828	0.9931	0.8376	0.9963	0.8312
71	0.8798	0.9891	0.8271	0.9976	0.8832	171	0.821	0.9928	0.8405	0.9959	0.8241
72	0.8163	0.9838	0.7408	0.9965	0.8196	172	0.812	0.9926	0.8136	0.9963	0.8157
73	0.7738	0.9804	0.6812	0.9961	0.7757	173	0.791	0.9917	0.7939	0.9958	0.7949
74	0.8742	0.9887	0.8184	0.9976	0.8776	174	0.84	0.9938	0.8252	0.9973	0.843
75	0.8799	0.9891	0.833	0.9973	0.8838	175	0.804	0.9922	0.8121	0.9959	0.8081
76	0.8622	0.9876	0.806	0.9971	0.866	176	0.816	0.9926	0.8367	0.9958	0.8198
77	0.8567	0.9873	0.7713	0.9985	0.8574	177	0.827	0.9933	0.8172	0.9969	0.8306
78	0.8612	0.9875	0.8059	0.997	0.8651	178	0.806	0.9922	0.8263	0.9956	0.8099
79	0.8221	0.9842	0.7603	0.9959	0.8269	179	0.811	0.9926	0.8038	0.9965	0.8147
80	0.888	0.9899	0.8387	0.9977	0.8913	180	0.8	0.992	0.8155	0.9956	0.8037
81	0.8799	0.9891	0.833	0.9973	0.8838	181	0.813	0.9927	0.8028	0.9966	0.8167
82	0.8408	0.986	0.7471	0.9984	0.8408	182	0.783	0.9916	0.7714	0.9961	0.7875
83	0.8866	0.9896	0.8595	0.9964	0.8914	183	0.828	0.9932	0.8322	0.9965	0.8312
84	0.8059	0.983	0.7247	0.9965	0.8087	184	0.782	0.9915	0.7805	0.9958	0.7867
85	0.8228	0.9845	0.701	0.9993	0.818	185	0.792	0.9916	0.8157	0.9952	0.7961
86	0.7921	0.9821	0.6727	0.9982	0.7884	186	0.861	0.9946	0.8408	0.9978	0.863
87	0.8005	0.9824	0.7382	0.9951	0.806	187	0.789	0.9917	0.789	0.9959	0.7936
88	0.8567	0.9871	0.8108	0.9963	0.8616	188	0.819	0.993	0.8082	0.9968	0.8228
89	0.834	0.9851	0.7859	0.9955	0.8396	189	0.823	0.993	0.8251	0.9965	0.8266
90	0.8752	0.9888	0.82	0.9976	0.8786	190	0.797	0.9918	0.8206	0.9953	0.801
91	0.7894	0.9817	0.696	0.9966	0.7907	191	0.804	0.9921	0.8259	0.9955	0.8074
92	0.8293	0.9849	0.7613	0.9965	0.8331	192	0.806	0.9922	0.8263	0.9956	0.8099
93	0.8514	0.9868	0.7575	0.9988	0.851	193	0.8	0.9923	0.7816	0.9966	0.8032
94	0.7967	0.9824	0.6917	0.9976	0.7958	194	0.791	0.9917	0.7939	0.9958	0.7949
95	0.8839	0.9895	0.835	0.9976	0.8875	195	0.804	0.9921	0.8218	0.9956	0.8083
96	0.8089	0.9833	0.7204	0.997	0.8106	196	0.801	0.9923	0.7816	0.9967	0.8045
97	0.8421	0.9858	0.7953	0.9957	0.8475	197	0.83	0.9934	0.8264	0.9968	0.8337
98	0.8927	0.9903	0.8326	0.9985	0.895	198	0.813	0.9927	0.8028	0.9966	0.8167
99	0.8336	0.985	0.7876	0.9954	0.8394	199	0.796	0.9921	0.7796	0.9965	0.8
100	0.8731	0.9886	0.8158	0.9976	0.8764	200	0.801	0.9924	0.7742	0.9969	0.8042
				<u>MCC</u>	<u>Accuracy</u>	<u>Sensitivity</u>	<u>Specificity</u>	<u>F-Score</u>			
Average				0.830923	0.9896	0.8	0.997	0.83405			

4. Conclusion

In this study, the important roles of detecting and diagnosing cold nodules has been discussed since they are known as high risk of infected by the thyroid cancer. The image pre-processing and processing techniques including image enhancement (grey level of blue channel, grey scale, logical negation and circular averaging filter), image segmentation (thresholding) were applied. These techniques couldn't solely capable of determining the cold nodules in thyroid radioisotope images so, a hill climbing algorithm was applied in order to automatic determination of these regions as it was much simpler than other

intelligent systems such as artificial neural networks, genetic algorithms, Fuzzy Support Vector Machines, as well as Support Vector Machines. Finally, the current approach was able to diagnose the cold nodules with high performance. From the results achieved in this study, one may deduce that, simple approaches are also capable of successfully reaching high performances in clinical realm.

Acknowledgments

None to declare.

References

- [1] C. Y. Chang, Y. F. Lei, C. H. Tseng, and S. R. Shih, "Thyroid segmentation and volume estimation in

- ultrasound images," *IEEE Trans Biomed Eng*, vol. 57, no. 6, pp. 1348-57, Jun, 2010.
- [2] P. W. Smith, *What You Must Know About Thyroid Disorders & What To Do About Them: Your Guide to Treating Autoimmune Dysfunction, Hypo- and Hyperthyroidism, Mood ... Loss, Weight Issues, Celiac Disease & More*, 1st ed.: Square One, 2016.
- [3] W. Mendre, and R. D. Raut, "Thyroid Disease Diagnosis using Image Processing: A Survey," *International Journal of Scientific and Research Publications*, vol. 2, pp. 1-4, 2012.
- [4] E. Alkım, E. Gürbüz, and E. Kılıç, "New intelligent diagnosis method to determine thyroid disorders." pp. 38-41.
- [5] A. Shukla, R. Tiwari, P. Kaur, and R. R. Janghel, "Diagnosis of Thyroid Disorders using Artificial Neural Networks." pp. 1016-1020.
- [6] A. Al Nofal, M. R. Gionfriddo, A. Javed, Q. Haydour, J. P. Brito, L. J. Prokop, S. T. Pittock, and M. H. Murad, "Accuracy of thyroid nodule sonography for the detection of thyroid cancer in children: systematic review and meta-analysis," *Clin Endocrinol (Oxf)*, vol. 84, no. 3, pp. 423-30, Mar, 2016.
- [7] C. A. Welch Dinauer, R. M. Tuttle, D. K. Robie, D. R. McClellan, R. L. Svec, C. Adair, and G. L. Francis, "Clinical features associated with metastasis and recurrence of differentiated thyroid cancer in children, adolescents and young adults," *Clin Endocrinol (Oxf)*, vol. 49, no. 5, pp. 619-28, Nov, 1998.
- [8] Y. E. Demidchik, V. A. Saenko, and S. Yamashita, "Childhood thyroid cancer in Belarus, Russia, and Ukraine after Chernobyl and at present," *Arq Bras Endocrinol Metabol*, vol. 51, no. 5, pp. 748-62, Jul, 2007.
- [9] B. Sokouti, S. Haghipour, and A. D. Tabrizi, "A pilot study on image analysis techniques for extracting early uterine cervix cancer cell features," *J Med Syst*, vol. 36, no. 3, pp. 1901-7, Jun, 2012.
- [10] M. Sokouti, and B. Sokouti, "ARTIFICIAL INTELLIGENT SYSTEMS APPLICATION IN CERVICAL CANCER PATHOLOGICAL CELL IMAGE CLASSIFICATION SYSTEMS — A REVIEW," *Biomedical Engineering: Applications, Basis and Communications*, vol. 28, no. 02, pp. 1630001, 2016.
- [11] B. Sokouti, S. Haghipour, and A. D. Tabrizi, "A framework for diagnosing cervical cancer disease based on feedforward MLP neural network and ThinPrep histopathological cell image features," *Neural Computing and Applications*, vol. 24, no. 1, pp. 221-232, January 01, 2014.
- [12] M. A. Devi, S. Ravi, J. Vaishnavi, and S. Punitha, "Classification of Cervical Cancer Using Artificial Neural Networks," *Procedia Computer Science*, vol. 89, pp. 465-472, 2016/01/01/, 2016.
- [13] M. M. Mehdy, P. Y. Ng, E. F. Shair, N. I. M. Saleh, and C. Gomes, "Artificial Neural Networks in Image Processing for Early Detection of Breast Cancer," *Comput Math Methods Med*, vol. 2017, pp. 2610628, 2017.
- [14] R. Guzmán-Cabrera, J. R. Guzmán-Sepúlveda, M. Torres-Cisneros, D. A. May-Arrijoa, J. Ruiz-Pinales, O. G. Ibarra-Manzano, G. Aviña-Cervantes, and A. G. Parada, "Digital Image Processing Technique for Breast Cancer Detection," *International Journal of Thermophysics*, vol. 34, no. 8, pp. 1519-1531, September 01, 2013.
- [15] S. Tsantis, D. Cavouras, I. Kalatzis, N. Piliouras, N. Dimitropoulos, and G. Nikiforidis, "Development of a support vector machine-based image analysis system for assessing the thyroid nodule malignancy risk on ultrasound," *Ultrasound Med Biol*, vol. 31, no. 11, pp. 1451-9, Nov, 2005.
- [16] R. C. Gonzalez, and R. E. Woods, *Digital Image Processing*, 3rd ed.: Pearson, 2007.
- [17] P. Dhaygude, and S. M. Handore, "A Review of Thyroid Disorder Detection Using Medical Images," *International Journal on Recent and Innovation Trends in Computing and Communication* vol. 2, pp. 4194-4197, 2014.
- [18] J. Xia, H. Chen, Q. Li, M. Zhou, L. Chen, Z. Cai, Y. Fang, and H. Zhou, "Ultrasound-based differentiation of malignant and benign thyroid Nodules: An extreme learning machine approach," *Computer Methods and Programs in Biomedicine*, vol. 147, no. Supplement C, pp. 37-49, 2017/08/01/, 2017.
- [19] Institute-of-Medicine-National-Research-Council, *Advancing Nuclear Medicine Through Innovation*, Washington, DC: The National Academies Press, 2007.
- [20] L. Goldman, and A. I. Schafer, *Goldman-Cecil medicine*, 2016.
- [21] P. Iranmanesh, M. Pusztaszeri, J. Robert, P. Meyer, B. Schiltz, S. M. Sadowski, M. O. Goumaz, and F. Triponez, "Thyroid Carcinoma in Hot Nodules: Review of the Literature," *World J Endoc Surg*, vol. 5, no. 2, pp. 50-54, 2013.
- [22] A. Torab, M. Sokouti, P. Rezaei, and S. Habibi, "Image processing technique for determining cold thyroid nodules," in 8th iranian conference on electrical and electronic engineering, https://www.civilica.com/Printable-ICEEE08_182=Image-processing-technique-for-determining-cold-thyroid-nodules.html, 2016, pp. 1-4.
- [23] J. Lever, M. Krzywinski, and N. Altman, "Points of Significance: Classification evaluation," *Nat Meth*, vol. 13, no. 8, pp. 603-604, 08/print, 2016.
- [24] A. Chaudhary, and S. S. Singh, "Lung Cancer Detection on CT Images by Using Image Processing." pp. 142-146.
- [25] R. Harrabi, and E. Ben Braiek, "Color image segmentation using multi-level thresholding approach and data fusion techniques: application in the breast cancer cells images," *EURASIP Journal on Image and Video Processing*, vol. 2012, no. 1, pp. 11, May 17, 2012.
- [26] G. Stockman, and L. G. Shapiro, *Computer Vision: Prentice Hall PTR*, 2001.
- [27] Q. Huang, W. Gao, and W. Cai, "Thresholding technique with adaptive window selection for uneven lighting image," *Pattern Recognition Letters*, vol. 26, no. 6, pp. 801-808, 2005/05/01/, 2005.

- [28] M. C. Frates, C. B. Benson, J. W. Charboneau, E. S. Cibas, O. H. Clark, B. G. Coleman, J. J. Cronan, P. M. Doubilet, D. B. Evans, J. R. Goellner, I. D. Hay, B. S. Hertzberg, C. M. Intenzo, R. B. Jeffrey, J. E. Langer, P. R. Larsen, S. J. Mandel, W. D. Middleton, C. C. Reading, S. I. Sherman, and F. N. Tessler, "Management of thyroid nodules detected at US: Society of Radiologists in Ultrasound consensus conference statement," *Radiology*, vol. 237, no. 3, pp. 794-800, Dec, 2005.
- [29] N. Singh, and A. Jindal, "A Segmentation Method and Comparison of Classification Methods for Thyroid Ultrasound Images," *International Journal of Computer Application*, vol. 50, no. 11, pp. 43-49, 2012.
- [30] I. Kononenko, "Estimating attributes: Analysis and extensions of RELIEF," *Machine Learning: ECML-94: European Conference on Machine Learning Catania, Italy, April 6-8, 1994 Proceedings*, F. Bergadano and L. De Raedt, eds., pp. 171-182, Berlin, Heidelberg: Springer Berlin Heidelberg, 1994.
- [31] C. Zhang, C. Sun, and T. D. Pham, "Segmentation of clustered nuclei based on concave curve expansion," *Journal of Microscopy*, vol. 251, no. 1, pp. 57-67, 2013.
- [32] S. J. Russell, and P. Norvig, *Artificial Intelligence: A Modern Approach*: Pearson Education, 2003.
- [33] B. Zheng, "Computer-Aided Diagnosis in Mammography Using Content-based Image Retrieval Approaches: Current Status and Future Perspectives," *Algorithms*, vol. 2, no. 2, pp. 828-849, 2009.

Massoud Sokouti obtained a Master of Science in Computer Engineering with a specialization in Computer Architecture from Department of Electrical and Computer Engineering at Shahid Beheshti University, Tehran, Iran and a Bachelor of Science in Information Technology Engineering with a specialization in IT from University of Tabriz, Tabriz, Iran. Currently, he is a PhD student in Nuclear Medicine with a specialization in Meta-Analysis at Nuclear Medicine Research Center, Mashhad University of Medical Sciences, Mashhad, Iran, and an excellent member of Computer Society of Iran. He has been awarded the first prize of scientific and technical innovation in 6th National Conference on Electronic Commerce and Economy and in National Conference in New Ideas in Electrical Engineering. He has worked on Microsoft SQL Server 2005, Net beans, Eclipse, MATLAB, and C++ programming. His main research is in the area of m-/e-commerce, cryptographic algorithms, network security, information security, wavelet, and genetic algorithms.

Mohsen Sokouti is a Professor at Department of Cardiothoracic Surgery of Tabriz University of Medical Sciences. He obtained his medical degree from University of Tehran, Iran. Then, he is specialized in general surgery and subspecialized in thoracic surgery at Tabriz University of Medical Sciences: Performs video-assisted thoracoscopic (VATS) and open surgery, esophageal, and mediastinal surgery with an emphasis on VATS lobectomy for treatment of lung cancer. Provides all facets of lung transplantation including donor management, donor/recipient selection, pre-operative work-up, surgery, and post-operative care.

Babak Sokouti is an Assistant Professor and has over 17 years IT technical management and consulting experience, including managing and maintaining sophisticated network infrastructures. He has obtained Bachelor of Science in Electrical Engineering with a specialization in Control from Isfahan University of Technology, Isfahan, Iran; a Master of Science in Electrical Engineering with a specialization in Electronics (with background of biomedical engineering) from Tabriz Branch, Islamic Azad University, Tabriz, Iran; a Master of Science in Information Security with Distinction from Royal Holloway University of London, London, UK; and obtained PhD in Bioinformatics from Biotechnology Research Center, Tabriz University of Medical Sciences, Tabriz, Iran. In addition, he has obtained IT industry certifications including MCP, MCSA 2003, MCDBA 2000, MCSE 2003, and MCTS 2008. His research interests include cryptographic algorithms, information security, network security and protocols, image processing, protein structure prediction, and hybrid intelligent neural network systems based on genetic algorithms.